# Mechanical Modeling of the Transcrystalline Interphase Behavior in Commingled PBT/Glass Fiber Composites

**J. VENDRAMINI, P. MELE, G. MERLE, AND N. D. ALBEROLA**

Laboratoire Matériaux Polymères et Composites, LMPC UMR CNRS 5041, Université de Savoie, Savoie Technolac, 73376 Le Bourget du Lac, France

*Received 2 August 1999; accepted 20 January 2000*

**ABSTRACT:** In a previous work, a mechanical model was proposed to predict the reinforcement of amorphous polymers by particulates as well as by unidirectional fibers over wide ranges of volume fractions of fillers and temperatures (or frequencies). This model is based on both the definition of a *representative morphological pattern* (RMP), accounting for the presence of fiber clusters, and a quantitative morphology analysis, based on the percolation concept. In this work, such an approach is extended to describe the viscoelastic properties of a semicrystalline polymer, poly(butylene terephthalate), commingled with 30 and 50 vol % of unidirectional glass fibers. It is found that aggregates constituted by both fiber clusters and a transcrystalline region (TCR) can act as the continuous phase. Based on the use of a mechanical model in a reverse mode, the actual viscoelastic behavior of this TCR is extracted and compared to that displayed by the unfilled polymer. © 2000 John Wiley & Sons, Inc. J Appl Polym Sci 77: 2513–2524, 2000

**Key words:** commingled polybutylene terephthalate/UD glass fiber composites; transcrystalline region; mechanical modeling; quantitative morphological analysis; percolation theory

## INTRODUCTION

It is well known that the mechanical properties of filled polymers are governed by both the reinforcement effect of the polymer matrix by fibers and by the physicochemical interactions at the polymer/fiber interface.[1–8]

The magnitude of the reinforcement effect in composites depends not only on the relative amount and properties of each phase but also on the filler spatial distribution within the matrix. In fact, clusters of fillers induce an improvement of the magnitude of the mechanical coupling between phases resulting in both a strong increase in the stiffness and a decrease in the damping factor.[4,9]

The interactions at the polymer/filler interface can be related to changes in the microstructure of the polymer at the vicinity of the fibers leading to the development of an interphase.[4,10] For example, in filled semicrystalline polymers, many workers[11–22] have observed the formation of a transcrystalline region (TCR) in the vicinity of fillers. Thus, Möginger et al.[11] revealed by polarized optical microscopy the presence of a transcrystalline layer around fillers in injection-molded poly(butylene terephthalate) (PBT)/short-glass fiber composites. Thomason and van Royen[21] showed that the growth of the transcrystalline region depends on a lot of key features, such as, for example, (i) the axial thermal expansion coefficient of the fiber, (ii) the sample cooling rate, (iii) the fiber length and the position along the fiber, and (iv) the polymer molecular weight.

*Correspondence to:* N. D. Alberola. E-mail: Alberola@univ-savoie.fr

Contract grant sponsor: Rhône-Alpes region.

Journal of Applied Polymer Science, Vol. 77, 2513–2524 (2000)

**Table I Characteristics of PolyButylene Terephtalate**

| Polymer | $\bar{M}_n$ (g/mol) | $\bar{M}_w$ (g/mol) |
|---|---|---|
| PBT | 37,000 | 81,000 |

In this work, it is proposed to assess the actual viscoelastic properties of the transcrystalline interphase in commingled PBT/unidirectional (UD) glass fibers, by assuming, to a first approximation, this interphase to be a well-defined third phase. This evaluation is based on both quantitative morphology analysis and mechanical modeling.

## EXPERIMENTAL

### Materials

The matrix used in this study is a semicrystalline thermoplastic polyester (i.e., PBT), provided by the Dupont de Nemours Company (Wilmington, NC, USA) under the trade name of Crastin 6131®. Its characteristics are reported in Table I.

Unidirectional glass fibers supplied by Vetrotex International have an average diameter of 17 $\mu$m. A specific coating agent based on saturated polyester is used for surface treatment. The fibers show elastic behavior over the temperature range studied. Shear modulus and Poisson's ratio are constant and equal to about 30 GPa and 0.2, respectively.[23]

### Sample Preparation

Composite specimens are processed by Vetrotex International and commercialized under the trade name of Twintex®.[24] Glass fibers are simultaneously commingled with PBT during the manufacture of Roving®.[25] The UD sheets are then pressed at 240°C under pressure and cooled at room temperature for about 40 min.

As the viscosity of used PBT is very low, unfilled polymer specimens cannot be processed by compression molding as composite materials. Accordingly, unfilled PBT samples are injection molded at 240°C and cooled in the mold at 20°C. Specimens are then heated at 120°C for 4 h to dry injected PBT specimens.[26]

Table II lists the characteristics of the composites reinforced by 30 and 50 vol % of UD fibers. In the next parts of the article, these will be referred to as 30 and 50% composites, respectively. Effective filler contents are determined from the residues of burned samples. The void content of composite samples is evaluated from density measurements.

### Test Procedures

Differential scanning calorimetry (DSC) is carried out over the temperature range from −50 to 120°C at a heating rate of 20°C/min by using a Perkin–Elmer DSC7 instrument purged with nitrogen gas. Thermograms are calibrated by using indium and octadecane. Glass transition, $T_g$, and melting point, $T_m$, temperatures are determined from the change in the slope of the baseline and the maximum of the melting peak, respectively. The crystallinity ratio, $X_c$, is determined through the following equation:

$$X_c = \frac{\Delta H_T}{\Delta H_\infty} \quad (1)$$

where $\Delta H_t$ is the area of the melting endotherm *per* gram of polymer and $\Delta H_\infty$ is the melting enthalpy of a perfect crystal of PBT, equal to 142 J/g.[27]

Scanning electron microscopy (SEM) observations are performed on the transversal area of polished and metallized samples by using a Phillips 525M scanning electron microscope. SEM micrographs are then digitalized by an image analyzer consisting of a video camera connected to a computer through a Matrox Meteor card. Images (512 × 512 8-bit pixels) are processed by means of software developed by the Reconnaissance des Forces et Visions Laboratory (INSA, Lyon, France).

Optical micrographs of composites are performed on thin slices of samples in transmission mode by using a Leitz microscope with crossed-polarizers.

**Table II Characteristics of the Commingled PBT/UD Glass Fiber Composites**

| Materials | Fiber Content (vol %) | Effective Fiber Content (vol %) | Porosity Content (%) |
|---|---|---|---|
| PBT/Glass fibers | 30 | 29.7 ± 0.5 | <1.0 |
| PBT/Glass fibers | 50 | 50.3 ± 0.5 | 3.0 |

**Table III DSC Characteristic Values of the Unfilled Polymer and Composite Materials**

| Materials | Fiber Content (vol %) | $T_g$ (°C) | $T_m$ (°C) | $X_c$ (%) |
|---|---|---|---|---|
| Non-reinforced PBT | 0 | 51.0 ± 1.0 | 224.5 ± 0.5 | 36.0 ± 2.0 |
| PBT/Glass fibers | 30 | 52.0 ± 1.0 | 224.5 ± 0.5 | 33.0 ± 2.0 |
| PBT/Glass fibers | 50 | 53.0 ± 1.0 | 224.5 ± 0.5 | 34.0 ± 2.0 |

Dynamic mechanical spectrometry analysis is carried out on unfilled PBT and composite materials by using a high-resolution inverted torsion pendulum (Micromechanalyser, Metravib, France). This setup provides the real ($G_{LT}'$) and imaginary ($G_{LT}''$) parts of the axial shear modulus $G_{LT}$ of the composites and the internal friction tan δ as a function of either the temperature (for one or several frequencies) or the frequency (under isothermal conditions). In this work, runs are performed by increasing the temperature from −20 to 120°C at 1 Hz and at a heating rate of 65°C/h. Mean dimensions of unfilled PBT and composites samples are close to 1.5 × 6 × 50 mm.

## RESULTS

### DSC Measurements

The characteristic values determined from the thermograms of the unfilled PBT and the polymer reinforced by 30 and 50 vol % of unidirectional glass fibers are listed in Table III.

In spite of the different processes used to elaborate the unfilled PBT and the composites, no significant changes in $T_g$ and $T_m$ nor in the overall crystallinity ratio ($X_c$) induced by fibers are detected by DSC measurements. However, this does not exclude possible local modifications of the microstructure of the polymer at the vicinity of fibers (e.g., the presence of a transcrystalline phase).

### SEM Observations and Image Analysis

Figure 1 shows the 2D geometric arrangement of fibers within matrix of composites reinforced by (a) 30 and (b) 50 vol % of fibers. For low as well as for high volume fractions of fillers, a lot of fibers are packed into clusters within which a part of the polymer is entrapped. Thus, at this analysis scale, these mesostructures seem to be limited on their outside by connected glass fibers.[4] In the next part of the article, the entrapped polymer is defined as the nonpercolated polymer and the rest of the matrix as the percolated one.

An iterative algorithm is then used to process the digital image to evaluate the content of percolated and nonpercolated polymer in 2D. Average values from the analysis of four images for each sample are reported in Table IV.[28]

### Quantitative Morphology Approach

On the basis of the percolation theory,[29,30] it is now of interest to determine the theoretical evo-

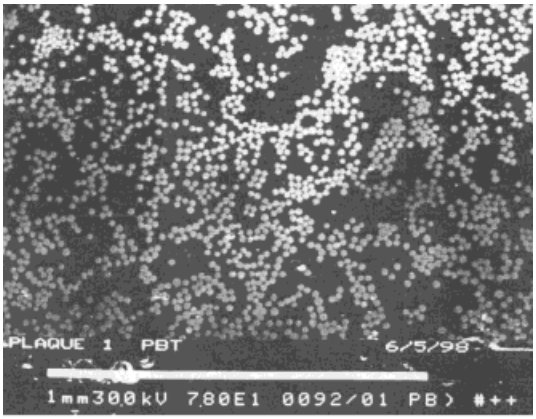


(a)

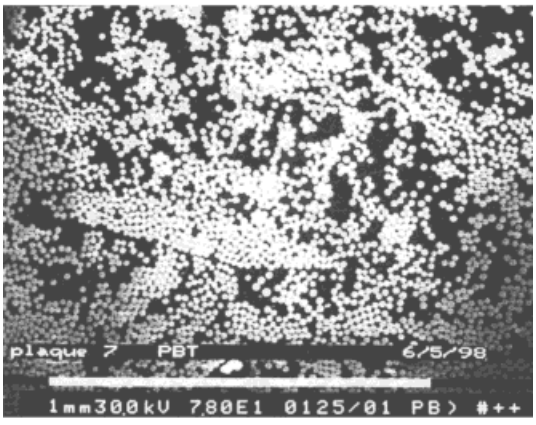


(b)

**Figure 1** SEM observations of 2D geometric arrangement of fillers in composites showing (a) 30 and (b) 50 vol % of glass fibers.

**Table IV Mean Volume Fractions of Fiber, Percolated Matrix, and Nonpercolated Polymer Determined from Image Analysis of the Composite Materials**

| Materials | Fiber Content (vol %) | Content of Percolated Polymer (vol %) | Content of Nonpercolated Polymer (vol %) |
|---|---|---|---|
| Unreinforced PBT | 0 | — | — |
| PBT/Glass fibers | 30 | 64.0 ± 1.0 | 6.0 ± 1.0 |
| PBT/Glass fibers | 50 | 37.0 ± 1.0 | 13.0 ± 1.0 |

lution of the volume fraction of effective matrix which actually contributes to viscoelasticity of the composite (i.e., the volume fraction of percolated matrix), versus the content of fiber by taking into account the experimental morphology analysis.

For fiber contents, $V_f$, ranging from 0 to the clustering threshold of fibers, $V_{fc}$, the volume fraction of percolated matrix, $V_{mp}$, is equal to the volume fraction of matrix:

$$V_{mp} = V_m = 1 - V_f \tag{2}$$

$V_{fc}$ is evaluated to be 0.1 from morphological analysis of the two composites through a method previously developed by Alberola et al.[4]

At the maximum packing fraction of fibers, $V_{f\max}$, a macroscopic phase inversion, occurs and $V_{mp} = 0$ for $V_m = V_{\min}$ with $V_{\min} = 1 - V_{f\max}$.

By increasing the volume fraction of glass fibers from the clustering threshold, $V_{fc}$, to $V_{f\max}$, the volume fraction of percolated matrix, obeys the percolation law which can be expressed by the following relationship:

$$V_{mp} = V_m\left[\frac{V_m - V_{\min}}{V_{cm} - V_{\min}}\right]^{\beta} \tag{3}$$

where $V_{cm} = 1 - V_{fc}$ and the critical exponent $\beta$ is 0.14 for the 2D lattice.[30]

Figure 2 shows the theoretical variations of the volume fraction of percolated matrix versus the content of glass fibers by considering $V_{f\max} = \pi/2\sqrt{3} \approx 0.91$ (i.e., the theoretical maximum packing fraction of disks in 2D). Experimental data from morphology analysis, accounting for uncertainties including porosity content, are also shown for comparison. It is clear that this law overestimates the volume fraction of percolated matrix over the analyzed range of filler content. In contrast, by taking $V_{f\max} = 0.55$ (and then $V_{\min} = 0.45$), theoretical volume fractions of percolated matrix are close to experimental data for the different composites. Such a result is in agreement with industrial findings for the commingling process. As a matter of fact, by this particular engineering process, the maximum amount of fibers able to be commingled with PBT matrix cannot exceed 60 vol %. Above this critical value, void content sharply increases, delamination occurs, and the composite properties rapidly diminish.

## Polarized Optical Microscopy Observations

Figure 3 exhibits polarized optical microscopy observations in a transmission mode of composites reinforced by (a) 30 and (b) 50 vol % of fibers, respectively.

In both composites, the polymer layer shell surrounding the fibers and the polymer entrapped within the clusters of fibers exhibit different birefringence from that of the rest of the matrix. The thickness of the interlayer shell can vary from 0 to 3 $\mu$m, according to the fiber content. In the following parts of the article, both the interphase and the occluded polymer will be then defined as the transcrystalline region (TCR). In the rest of

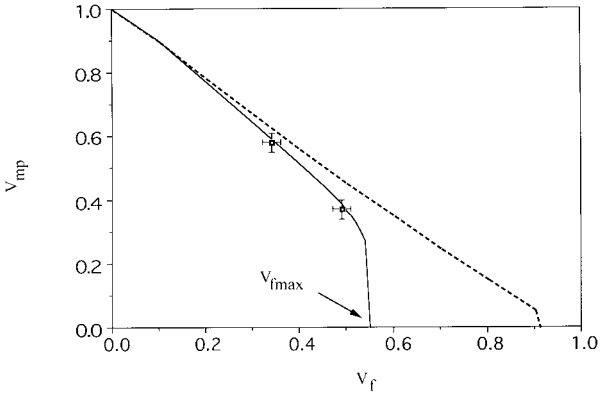


**Figure 2** Theoretical variations of the volume fraction of percolated matrix, $V_{mp}$, versus the volume fraction of fibers, $V_f$. Experimental results from quantitative image analysis for both composites (□).

the matrix, well-defined spherulites can be distinguished.

### Dynamic Mechanical Spectrometry

Figure 4 shows the experimental variations of (a) $G_{LT'}$ and (b) tan δ versus temperature for unfilled PBT and composites reinforced by 30 and 50 vol % of glass fibers.

The increase of the axial shear modulus over the analyzed temperature range accompanied by the decrease of the maximum damping factor displayed by the two composites can be attributed not only to the usual reinforcement effect induced by fibers, but also to an enhancement of the mechanical coupling effect due to the presence of fiber aggregates.[4] In addition, it is expected that the presence of a TCR can affect the overall viscoelasticity of composites. As a matter of fact, the TCR developed at the vicinity of the fibers can exhibit mechanical properties along the fibers different from those displayed in the transverse direction. Furthermore, a significant shift of the main relaxation, $T_\alpha$, toward the lower temperatures shown by the 30% composite can be noted. This temperature shift of the $T_\alpha$ relaxation is not detected for the 50% composite. In fact, the tan δ maximum displayed by this composite is located at about the same temperature as that recorded for the unfilled polymer.

The unexpected behavior displayed by the 30% composite can then result from the two following origins. (i) Some changes in the microstructure of the polymer at the vicinity of fibers involve an increase in the molecular motion ability of chains in the amorphous phase of TCR. (ii) The relaxation of some internal stresses can originate on cooling from the processing temperature due to the different thermal expansion coefficients of polymer and glass fibers. The differences between viscoelasticity displayed by both composites will be discussed later.

### Mechanical Properties of the TCR

The aim of this work is now to evaluate the characteristics of the TCR, assumed to be a well-defined third phase, to a first approximation. To reach this aim, it is first required to recall the main morphological characteristics of composites determined from the previous analysis. Thus, we put forward the following working data:

(i) Fibers show a transcrystalline layer the thickness of which varies according to the filler content. For the 30% composite, the interphase thickness, $e$, ranges from 0 to 3 μm, whereas $e < 1$ μm for the highest filled polymer. (ii) Layered fibers are packed into clusters. (iii) Polymer entrapped within the clusters shows the same microstructure as the layer shell and then it can exhibit the same mechanical properties. The second step implies a definition of a representative morphological pattern of such a kind of composite to predict the viscoelastic properties of the interphase through a self-consistent scheme. As the occluded polymer is assumed to have the same mechanical properties as those of the interphase, the composite materials can now be considered as follows: aggregates of layered fibers including the polymer entrapped within the cluster are considered as the reinforcing phase of the rest of the polymer, the so-called *unmodified polymer* ($V_m$). The volume fraction of the reinforcing phase, $V_{RP}$, can be expressed by:

$$V_{RP} = V_{Lf} + V_{EP} = 1 - V_m \tag{4}$$

where $V_{Lf}$ is the volume fraction of layered fibers, $V_{EP}$ is the volume fraction of entrapped polymer, $V_m$ is the volume fraction of unmodified polymer, and $V_{Lf}$ can be defined through the following equation:

$$V_{Lf} = V_f\left[1 + \frac{e}{r_f}\right]^2 \tag{5}$$

where $V_f$ is the actual volume fraction of fibers, $r_f$ is the mean radius of glass fibers (~ 8.5 μm), and $e$ is the layer shell thickness.

Furthermore, it is expected that the characteristic parameters of the morphology are the same, whatever the analysis scale may be. Accordingly, $V_{EP}$ can be evaluated through the percolation law by replacing $V_f$ by $V_{Lf}$ and by assuming that the clustering threshold ($V_{fc}$) and the maximum packing fraction of layered fibers ($V_{f\max}$) are identical to those defined for raw fibers. The critical volume fraction, $V_{RPc}$, at which a macroscopic phase inversion occurs, is taken equal to 0.55, according to the multiscale approach. Subsequently, for $V_{RP} \geq 0.55$, aggregates act as the continuous phase and the unmodified polymer is entrapped within the interstices of the aggregates network. In contrast, for $V_{RP} < 0.55$, the continuous phase is the unmodified polymer ($V_m > 0.45$).

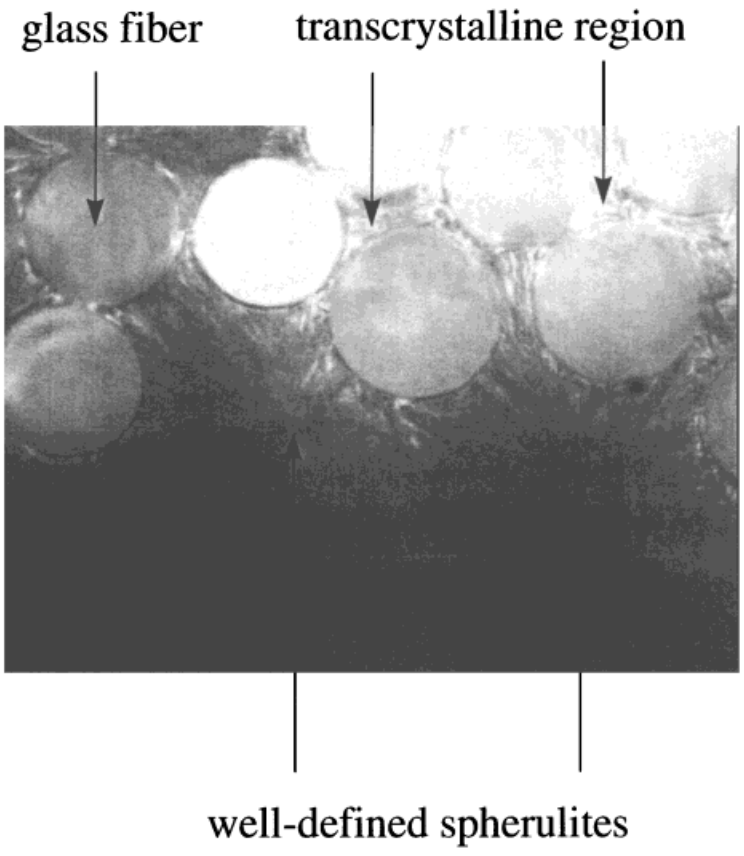
glass fiber
transcrystalline region
well-defined spherulites

(a)

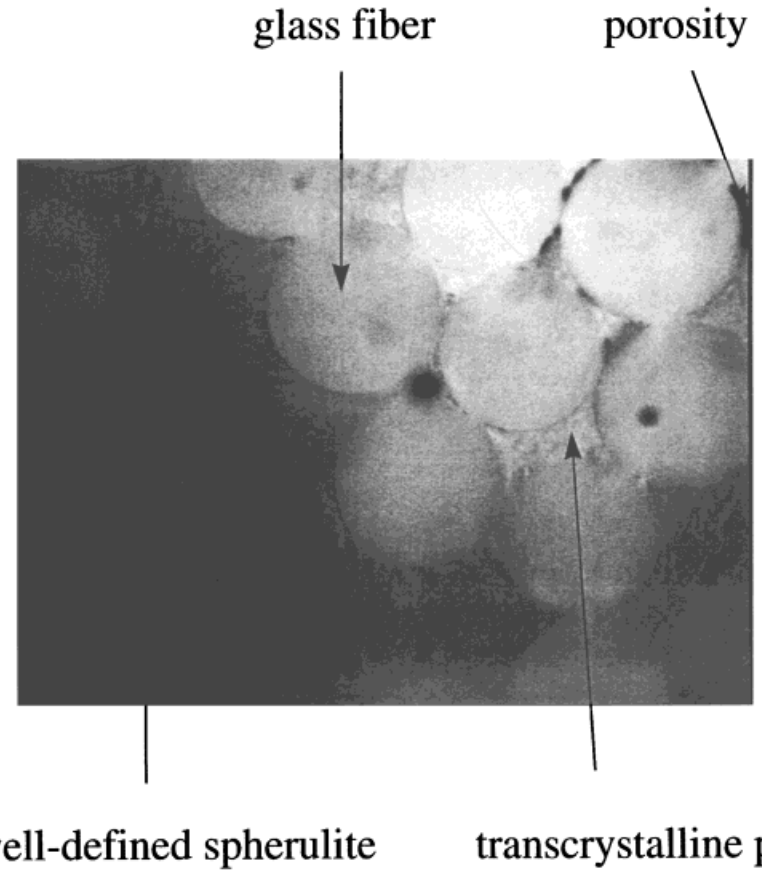
glass fiber
porosity
well-defined spherulite
transcrystalline phase

(b)

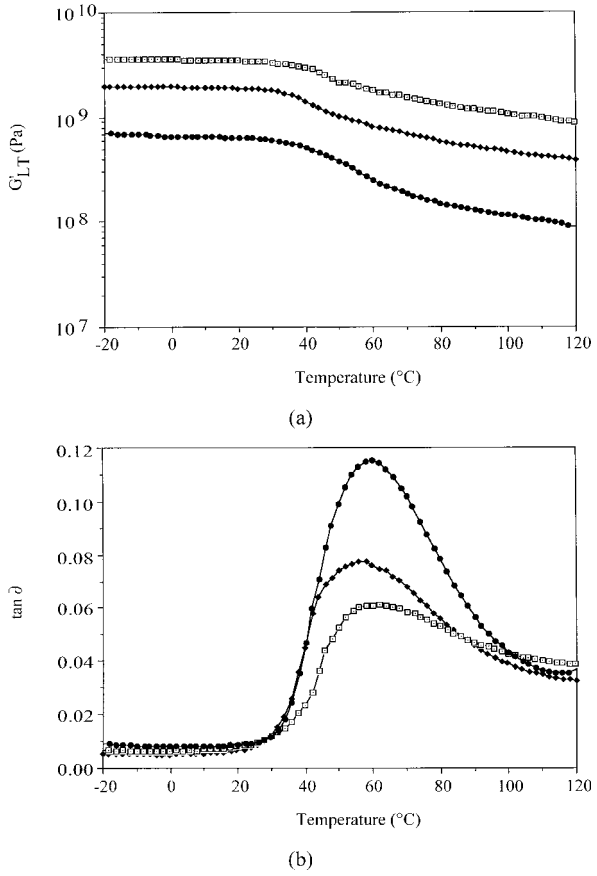


**Figure 4** Experimental variations of (a) $G_{LT}'$ and (b) tan δ versus temperature at 1 Hz for composites filled by 30 vol % (♦) and 50 vol % (□) of glass fibers. Data for unfilled polymer (●)

The volume fractions of layered fibers ($V_{Lf}$), entrapped polymer ($V_{EP}$), the reinforcing phase ($V_{RP}$), and the unmodified polymer ($V_m$) for various interphase thicknesses are listed in Table V for the 30% composite.

The interphase thickness cannot be higher than 3.0 μm in the lowest filled composite because the maximum packing fraction of layered fibers cannot exceed 0.55, as previously mentioned. Subsequently, for interphase thickness, $e$, ranging from 1.9 to 3.0 μm, it can be observed that $V_{RP} \geq V_{RPc}$ (=0.55). For this thickness range, aggregates then act as the continuous phase. In contrast, for interphase thicknesses lower than 1.9 μm, $V_{RP} < 0.55$ and then the continuous phase is the unmodified polymer.

For composites reinforced by 50 vol % of glass fibers, Table VI lists $V_{Lf}$, $V_{EP}$, $V_{RP,}$ and $V_M$ values for various interphase thicknesses.

For the highest reinforced composite, the maximum interphase thickness is equal to 0.4 μm. Accordingly, this can indicate that aggregates act as the continuous phase in such a composite, whatever the interphase thickness.

On the basis of these morphological considerations, it is now of interest to evaluate the average viscoelastic properties of the TCR. It is first required to separate the mechanical behavior of aggregates constituted by both clusters of layered fibers and entrapped polymer. This *extraction* can be performed by using a self-consistent scheme in a reverse mode. For volume fractions of aggregates $< V_{RPc}$ (=0.55), the representative morphological pattern (RMP) is constituted by a two-layered cylindrical inclusion in which aggregates is the central cylinder (phase 1) surrounded by the shell of unmodified polymer (phase 2), which acts as the continuous phase [Fig. 5(a)]. This RMP is characteristic of the morphology of composites reinforced by 30 vol % of UD fibers layered by an interphase thickness lower than 1.9 μm.

For volume fractions of aggregates $> 0.55$, the corresponding RMP is also a two-layered cylindrical inclusion, but the unmodified polymer (phase 1) is now embedded within the shell of aggregates (phase 2), which acts as the continuous phase [Fig. 5(b)]. This RMP can be used to describe the 30% composite showing an interphase thickness ranging from 1.9 to 3.0 μm. The description of the mechanical behavior of the 50% composite can be performed through an equivalent RMP, whatever the interphase thickness is. Thus, the viscoelastic properties of aggregates can be extracted by the use of the well-known three-phase model developed by Christensen and Lo in a reverse mode,[4,31–33] whatever both the fiber content and the interphase thickness are. Such a modeling requires the knowledge of the viscoelastic behavior of both unfilled PBT and composite materials. According to Hashin,[34,35] the expressions developed for isotropic elastic phases remain valid in the case of phases which are themselves trans-

**Figure 3** Polarized optical microscopy observations of composites reinforced by (a) 30 and (b) 50 vol % of UD fibers.

**Table V Volume Fractions of Layered Fibers, $V_{Lf}$, Entrapped Polymer, $V_{EP}$, Reinforcing Phase, $V_{RP}$, and Unmodified Polymer, $V_m$, Versus Interphase Thickness for the 30% Composite**

| Material | $V_f$ (vol %) | $e$ ($\mu$m) | $V_{Lf}$ (vol %) | $V_{EP}$ (vol %) | $V_{RP}$ (vol %) | $V_m$ (vol %) |
|---|---|---|---|---|---|---|
| PBT/Glass fibers | 30 | 1.0 | 38 | 8 | 46 | 54 |
| | 30 | 1.9 | 45 | 10 | 55 | 45 |
| | 30 | 2.0 | 46 | 11 | 57 | 43 |
| | 30 | 3.0 | 54 | 19 | 73 | 27 |

versely isotropic about an axis in the fiber direction.

Figure 6 shows the theoretical evolution of the glassy axial shear modulus of aggregates $G_{\mathrm{LTAV}}'$ separated from the viscoelastic behavior of the 30% composite versus the interphase thickness.

Two regions can be distinguished. (i) For an interphase thickness ranging from 0 to 1.9 $\mu$m (i.e., when aggregates act as the dispersed phase), the theoretical $G_{\mathrm{LTAV}}'$ strongly decreases with increasing $e$. Moreover, for an interphase thickness lower than about 0.6 $\mu$m, $G_{\mathrm{LTAV}}'$ would be greater than the axial shear modulus of raw glass fibers (30 GPa). This has no physical meaning. Accordingly, $e$ is necessarily $> 0.6$ $\mu$m for the 30% composite. (ii) For $e = 1.9$ $\mu$m, a macroscopic phase inversion occurs and it leads to the drop in the axial shear modulus of aggregates. With interphase thickness increasing from 1.9 to 3.0 $\mu$m (i.e., when aggregates act as the continuous phase), $G_{\mathrm{LTAV}}'$ slowly decreases.

For the 50% composite (e.g., when aggregates act as the continuous phase whatever value $e$ takes), Figure 7 shows that the glassy axial shear modulus of the aggregates slowly decreases with increasing the interphase thickness and always remains $< 30$ GPa.

It is now of interest to show the viscoelastic behavior of aggregates over the analyzed temperature range. For example, Figures 8 and 9 give the evolutions of $G_{\mathrm{LTA}}'$ and tan $\delta_A$, respectively, versus temperature of aggregates from composites reinforced by 30 and 50 vol % of UD fibers. Interphase thicknesses are chosen equal to 2.0 and 0.2 $\mu$m, respectively. Also shown for comparison are the dynamic mechanical properties of the unfilled polymer.

For all filler contents, both kinds of aggregates exhibit a weak drop in $G_{\mathrm{LTA}}'$ accompanied by a broad relaxation. Moreover, it can be noted that the maximum in the damping factor displayed by aggregates derived from the dynamic mechanical behavior of the 30% composite is located at a lower temperature than that displayed by the highest filled composite. Possible explanations of such behavior will be discussed later.

Now, by assuming to a first approximation that the mechanical behavior of the TCR is transversely isotropic, the viscoelastic properties of such a phase can be separated from the dynamic mechanical behavior of aggregates by using Christensen and Lo's model in a reverse mode. In fact, if the dynamic mechanical behavior of both aggregates and fibers is known, the theoretical viscoelastic properties of TCR can be evaluated by using a self-consistent scheme in a reverse mode extended to transversely isotropic properties of phases. The RMP is then constituted by a two-layered cylindrical inclusion in which phase 1 is

**Table VI Volume Fractions of Layered Fibers, $V_{Lf}$, Entrapped Polymer, $V_{EP}$, Reinforcing Phase, $V_{RP}$, and Unmodified Polymer, $V_m$, Versus Interphase Thickness for the 50% Composite**

| Material | $V_f$ (vol %) | $e$ ($\mu$m) | $V_{Lf}$ (vol %) | $V_{EP}$ (vol %) | $V_{RP}$ (vol %) | $V_m$ (vol %) |
|---|---|---|---|---|---|---|
| PBT/Glass fibers | 50 | 0.0 | 50 | 13 | 63 | 37 |
| | 50 | 0.2 | 52 | 16 | 68 | 32 |
| | 50 | 0.4 | 54 | 19 | 73 | 27 |
| | 50 | 0.7 | 59 | — | — | — |
| | 50 | 1.0 | 62 | — | — | — |

the raw glass fibers, which act as the dispersed phase, and phase 2 is the TCR (Fig. 10).

Plots of theoretical axial shear modulus, $G_{LTCR}'$, and damping factor, tan $\delta_{TCR}$, for the transcrystalline region versus temperature are shown in Figures 11 and 12, respectively.

Issues raised by the analysis of the theoretical spectra are the following:

(i) Over the analyzed temperature range, the axial shear moduli of the TCR separated from both composites are very close for the chosen TCR thicknesses and significantly greater than that displayed by the unfilled PBT. For example, the glassy modulus at −20°C and the *rubbery* modulus at 120°C of both TCRs are about 1.1 and 0.32 GPa, respectively, whereas corresponding values for the unfilled polymer are about 0.70 and 0.09 GPa.

Accordingly, it can be concluded that the stiffness along the fiber of such a transversely isotropic phase is greater than that of bulk polymer. As a matter of fact, according to Klein et al.,[13,17] the effective preferred orientation of the TCR would be that in which the *c*-axis of crystallites is aligned parallel to the fiber direction. Such an interpretation does not exclude the possible higher crystallinity ratio displayed by TCR with respect to that of bulk polymer.

(ii) The relaxation related to $T_g$ of TCR derived from the 30% composite is located at a temperature lower than that displayed by the unfilled polymer. This is accompanied by a temperature shift toward the lower temperatures of the onset of the $\alpha$ relaxation. In contrast, no significant changes in the temperature locations of the $T_\alpha$ and the onset of TCR for the 50% composite are detected.

As previously discussed, both the unexpected behavior displayed by TCR from the 30% composite and the differences between viscoelasticity exhibited by the interphase regions in the two composites could be related to several key features capable of acting in the same or in opposite ways, as for example,

- The relaxation of some residual stresses, induced by the thermal history of the composites, concentrated in the interphase regions;
- Changes in the molecular mobility of the amorphous phase in TCR due to modifications in the crystallite sizes which act as the physical ties;
- The influence of the TCR growth on the magnitude of the residual internal stresses. According to Klein and Marom,[17] internal stresses could be relieved by the preferred orientation growth of TCR relative to the fiber.
- The influence of the surface area of fiber/polymer interface and the interfiber distances on nucleation and growth phenomena of TCR, respectively.

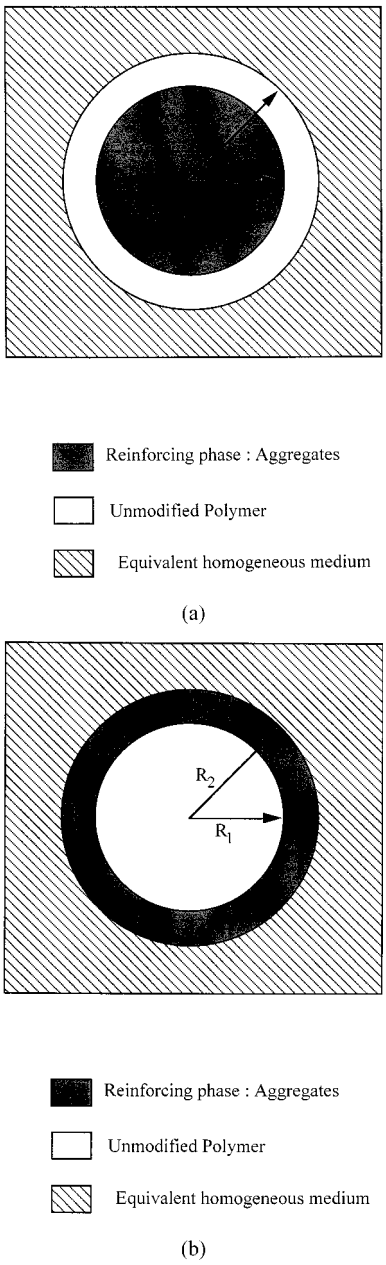


**Figure 5** Representative morphological patterns: a two-layered cylindrical inclusion embedded in the equivalent homogeneous medium. (a) Phase 1 is the aggregates and phase 2 is the unmodified polymer. (b) Phase 1 is the unmodified polymer and phase 2 is the aggregates.

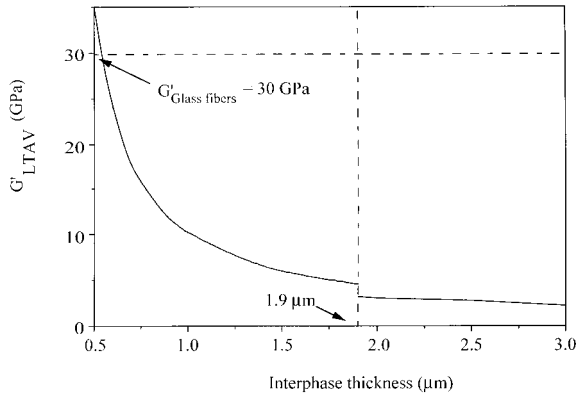


**Figure 6** Theoretical curve of the real part of the *vitreous* axial shear modulus $G_{LTAV}'$ of aggregates versus interphase thickness, *e*, for the composite reinforced by 30 vol % of glass fibers.

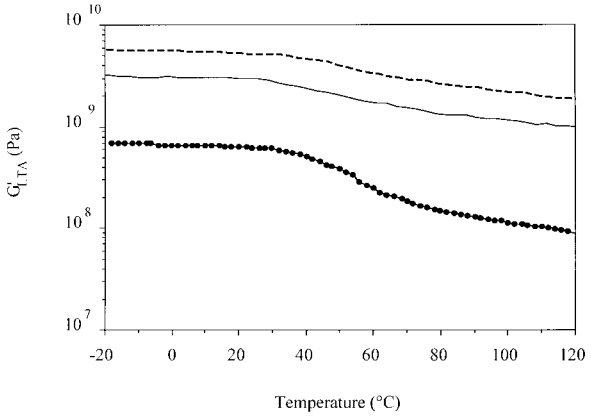


**Figure 8** Theoretical curve of the real part of the axial shear modulus of aggregates, $G_{LTA}'$ versus temperature for the composites reinforced by (—) 30 and (- - -) 50 vol % of glass fibers. Experimental results for the unfilled polymer are indicated by the filled circles (●).

## CONCLUSIONS

Based on both quantitative morphology analysis and the percolation concept, the viscoelastic behavior of the TCR in PBT commingled with UD glass fibers has been investigated.

From the morphological approach, it has been shown that (i) fibers are packed into clusters and (ii) the polymer entrapped within clusters and at the vicinity of glass fibers, defined as the TCR, exhibits a different birefringence from that of the rest of the matrix. Thus, the composites can be described as a two-phase material (i.e., an unmodified polymer showing well-defined spherulites), and aggregates consisting of the entrapped polymer and layered fibers.

The evaluation of the viscoelastic behavior of the transcrystalline region is then performed in two steps. In the first step, the dynamic mechanical behavior of aggregates, assumed to exhibit transversely isotropic properties, is extracted by using Christensen and Lo's model in a reverse mode. It is then required to define the phase acting as the continuous medium. From quantitative morphology analysis, it is shown that a macroscopic phase inversion occurs for a critical content of aggregates = 0.55. Such a value appears to be a characteristic signature of the process involved. Thus, in the composite

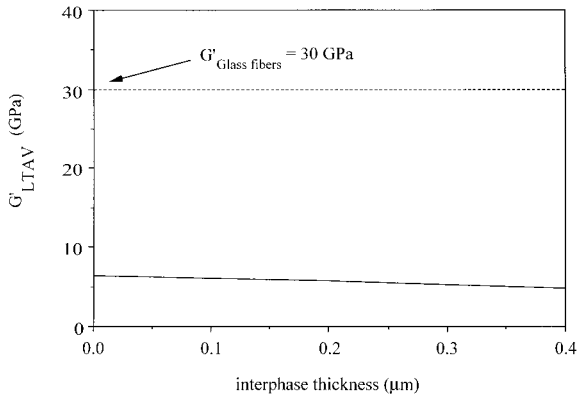


**Figure 7** Theoretical variations of the real part of the vitreous axial shear modulus $G_{LTAV}'$ of aggregates versus interphase thickness, *e*, for the composite filled by 50 vol % of UD fibers.

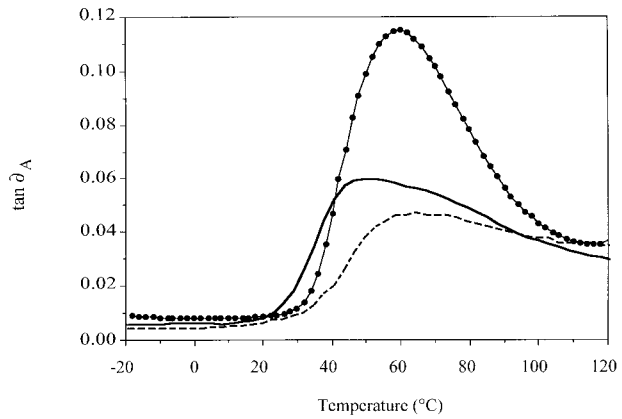


**Figure 9** Theoretical variations of the damping factor of aggregates, tan $\delta_A$, versus temperature for the composites reinforced by (—) 30 and (- - -) 50 vol % of glass fibers. Experimental results for the unfilled polymer are indicated by the filled circle (●).

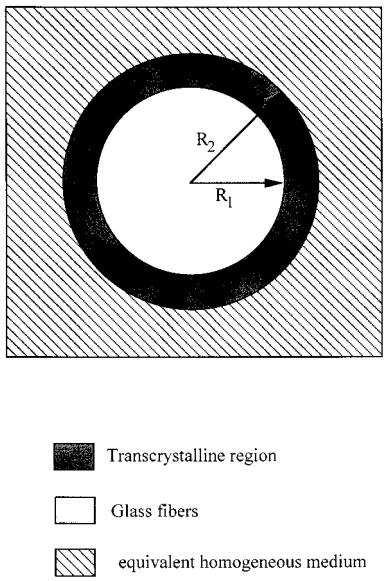


**Figure 10** Representative morphological pattern: a two-layered cylindrical inclusion embedded in the equivalent homogeneous medium. Phase 1 is the raw glass fibers and phase 2 is the transcrystalline region.

reinforced by 30 vol % of UD glass fibers, aggregates act as the continuous phase for interphase thickness $> 1.9$ $\mu$m. For the 50% composite, aggregates are the continuous phase whatever the interphase thickness.

In a second step, based on microscopic optical observations supported by Klein and Marom works,[17] the transcrystalline region is assumed to exhibit transversely isotropic properties. Viscoelasticity of such a phase can be separated from the behavior of the aggregates by invoking again the Christensen and Lo's model in a reverse mode. The relaxation spectra of TCR found is characterized by the two following features:

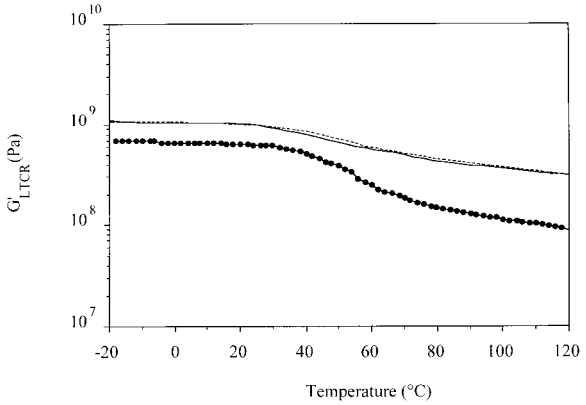


**Figure 11** Theoretical curve of the real part of the axial shear modulus of the transcrystalline region, $G_{LTCR}'$, versus temperature for the composites reinforced by (—) 30 and (- - -) 50 vol % of glass fibers. Experimental results for the unfilled polymer are shown by the filled circles (●).

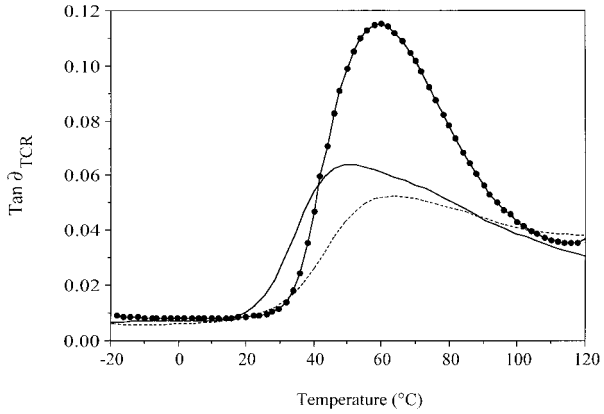


**Figure 12** Theoretical variation of the damping factor of the transcrystalline region tan $\delta_{TCR}$ versus temperature for the composites reinforced by (—0) 30 and (- - -) 50 vol % of glass fibers. Experimental results for the unfilled polymer are indicated by the filled circles (●).

(i) For the chosen interphase thickness (i.e., 2.0 and 0.2 $\mu$m, respectively), the axial shear modulus of TCR separated from the 30 and 50% composites are very close and higher than that exhibited by the unfilled polymer over the analyzed temperature range. This is consistent with the preferred orientation growth of TCR in which the *c*-axis of crystallites is probably aligned parallel to the fiber direction. This cannot exclude the possibility that TCR can exhibit a higher crystallinity ratio than that of unfilled PBT.

(ii) The changes in the location of the $T_\alpha$ relaxation of TCR, as displayed when increasing the fiber content from 30 to 50%, could be related to several key features including the relaxation of internal stresses and changes in the microstructure of the polymer at the vicinity of fibers, the latter of which could depend on both the surface area of interface and the interfiber distances.

This work was financially supported by the Rhône-Alpes region. Acknowledgments are also made to Vetrotex International (Chambéry–France) for the purchase of the materials used. The contribution of M. P. Boissonnat (Vetrotex International) was greatly appreciated for help in this project.

## NOMENCLATURE

$V$ = volume fraction of the different phases
$m$, $mp$, $f$ = subscript referring, respectively, to the polymer matrix, the percolated matrix, and the fibers
$V_{fc}$ = clustering threshold
$V_{c\min}$ = critical volume fraction of polymer at the clustering threshold
$V_{f\max}$ = maximum packing fraction of fibers
$V_{\min}$ = Minimum volume fraction of polymer
$V_{Lf}$ = volume fraction of layered fibers
$V_{RP}$ = volume fraction of the reinforcing phase
$V_{EP}$ = volume fraction of entrapped polymer
$r_f$ = radius of fibers
$e$ = interphase thickness
$G_{\mathrm{LT}}'$ = real part of the axial shear modulus of composite materials
$\tan \delta$ = damping factor of composite materials
$G_{\mathrm{LTAV}}'$ = real part of the *vitreous* axial shear modulus of aggregates
$G_{\mathrm{LTA}}'$ = real part of the axial shear modulus of aggregates
$\tan \delta_A$ = damping factor of aggregates
$G_{\mathrm{LTCR}}'$ = real part of the axial shear modulus of the transcrystalline region
$\tan \delta_{\mathrm{TCR}}$ = damping factor of the transcrystalline region

## REFERENCES


1. Thomason, J. L. Polym Comp 1990, 11, 105.
2. Park, H. J.; Ho, K. I.; Chun, B. C. J Korean Fiber Soc 1997, 34, 358.
3. Shan, H. Z.; Chou, T. W. Compos Sci Technol 1995, 53, 383.
4. Alberola, N. D.; Merle, G.; Benzarti, K. Polymer 1999, 40, 315.
5. Bonfield, S. J.; Berger, M. H.; Bunsell, A. R.; Watts, J. F.; Greaves, S. J.; Grosjean, F.; Rosenberg, E.; Bain, J. M. Polym Compos 1992, 5, 161.
6. Bergeret, A.; Alberola, N. Polymer 1996, 37, 2759.
7. Lewis, T. B.; Nielsen, L. E.; J Appl Polym Compos 1970, 17, 1449.
8. Tregub, A.; Harel, H.; Marom, G. J Mater Sci Lett 1994, 13, 329.
9. Mele, P.; Alberola, N. D. Compos Sci Technol 1996, 56, 849.
10. Theocaris, P. S. in The Concept and Properties of Mesophase in Composites; Ishida, H.; Koenig, J. L., Eds., Composite Interface: Berlin, Germany, 1986.
11. Möginger, B.; Müller, U.; Eyerer, P. Composites 1991, 22, 432.
12. Nagae, S.; Otsuka, Y.; Nishida, M.; Shimizu, T.; Takeda, T.; Yumitori, S. J Mater Sci Lett 1995, 14, 1234.
13. Klein, N.; Marom, G.; Pegoretti, A.; Migliaresi, C. Composites 1995, 26,707.
14. Hata, T.; Oshaka, K.; Yamada, T.; Nakamae, K.; Shibita, N.; Matsumoto, T. J Adhes 1994**,** 45, 125.
15. Avella, M.; Della Volpe, G.; Martuscelli, E.; Raimo, M. Polym Eng Sci 1992, 32, 376.
16. Blundell, J.; Crick, R. A.; Fife, B.; Peacock, J.; Keller, A.; Waddon, A. J Mater Sci 1989, 34, 2057.
17. Klein, N.; Marom, G. Composites 1994, 25, 706.
18. Klein, N.; Selivansky, D.; Marrom, G. Polym Compos 1995, 16, 189.
19. Reinsch, V. E.; Rebenfeld, L. Polym Compos 1992, 13, 353.
20. Thomason, J. L.; van Rooyen, A. A. J Mater Sci 1992, 27, 889.
21. Thomason, J. L.; van Rooyen, A. A. J Mater Sci 1992, 27, 897.
22. Moon, C. K. J Appl Polym Sci 1998, 67, 1191.
23. Wypych, G. Handbook of Fillers; Plastics Design Library: Toronto–New York, 1999.
24. Boyce, G. S. Composites 1997, 22, 35.
25. Wakeman, M. D.; Cain, T,. A. Rudd, C. D.; Brooks, R.; Long, A. C. Compos Sci Technol 1998, 58, 1879.
26. Jadhar, J. Y. Encyclopedia of Polymer Science and Engineering, 2nd ed., Vol. 12; Wiley: New York, 1988.
27. Nichols, M. E.; Robertson, R. E. J Polym Sci 1992, B30, 755.
28. Coster, C. J. L. Précis d'Analyse d'Images; Presses du CNRS: Washington, DC, 1989.
29. de Gennes, P. G. Scaling Concepts in Polymer Physics; Cornell University Press: Ithaca, NY, 1979.
30. Stauffer, D. Introduction to Percolation Theory; Taylor and Francis: London, 1985.
31. Colombini, D.; Merle, G.; Alberola, N. D. J Macro Sci Phys to appear.
32. Christensen, R. M.; Lo, K. H. J Mech Phys Solids 1979, 27, 315.
33. Christensen, R. M.; Lo, K. H. J Mech Phys Solids 1986, 34, 639.
34. Hashin, Z.; Int J Solids Struct 1970, 6, 797.
35. Hashin, Z. J Appl Mech 1979, 46, 543.